



ELSEVIER

Contents lists available at ScienceDirect

Journal of Theoretical Biology

journal homepage: www.elsevier.com/locate/yjtbi

Extra precision docking, free energy calculation and molecular dynamics simulation studies of CDK2 inhibitors

Sunil Kumar Tripathi^a, Ravikumar Muttineni^b, Sanjeev Kumar Singh^{a,*}^a Computer Aided Drug Designing and Molecular Modeling Lab, Department of Bioinformatics, Alagappa University, Karaikudi-630 003, Tamil Nadu, India^b Schrodinger, Bangalore 560079, India

HIGHLIGHTS

- Computational approach was applied to gain insight into selectivity for CDK2 inhibitors.
- These theoretical approaches reproduced the crystal structure precisely.
- The modification with substituents can show improved inhibitory activity against CDK2.

ARTICLE INFO

Article history:

Received 27 August 2012

Received in revised form

17 May 2013

Accepted 20 May 2013

Available online 29 May 2013

Keywords:

Cell-cycle

Glide XP docking

MM-GBSA

Binding free energy

Biological activity

ABSTRACT

Molecular docking, free energy calculation and molecular dynamics (MD) simulation studies have been performed, to explore the putative binding modes of 3,5-diaminoindazoles, imidazo(1,2-*b*)pyridazines and triazolo(1,5-*a*) pyridazines series of Cyclin-dependent kinase (CDK2) inhibitors. To evaluate the effectiveness of docking protocol in flexible docking, we have selected crystallographic bound compound to validate our docking procedure as evident from root mean square deviations (RMSDs). We found different binding sites namely catalytic, inhibitory phosphorylation, cyclin binding and CKS-binding site of the CDK2 contributing towards the binding of these compounds. Moreover, correlation between free energy of binding and biological activity yielded a statistically significant correlation coefficient. Finally, three representative protein–ligand complexes were subjected to molecular dynamics simulation to determine the stability of the predicted conformations. The low value of the RMSDs between the initial complex structure and the energy minimized final average complex structure suggests that the derived docked complexes are close to equilibrium. We suggest that the phenylacetyl type of substituents and cyclohexyl moiety make the favorable interactions with a number of residues in the active site, and show better inhibitory activity to improve the pharmacokinetic profile of compounds against CDK2. The structure-based drug design strategy described in this study will be highly useful for the development of new inhibitors with high potency and selectivity.

© 2013 Elsevier Ltd. All rights reserved.

1. Introduction

Cyclin-dependent kinases (CDKs) are serine/threonine kinases which control the proliferation of eukaryotic cell. Due to their crucial role in the regulation of the cell division cycle, CDKs have emerged as important therapeutic targets in anti-cancer drug research. The Cyclin-dependent kinase 2 (CDK2) is one of the prominent cell cycle regulators, which is dominantly active during the G1 phase and G1/S transition. The deregulation of CDKs is known to be associated with many serious diseases, such as cancer (Morgan, 1997; Malumbres and Barbacid, 2009; Child et al., 2010; Singh et al., 2012). This fact has attracted attention in the long term to the development of efficient inhibitors of CDKs (Besson

et al., 2008). Many government organizations and pharmaceutical companies have engaged in programs aiming at the discovery of potent small molecule inhibitors of these enzymes which are firmly established targets in oncology. A relentless effort in this field has succeeded in bringing some CDK inhibitors to clinical trials (Meijer and Raymond, 2003; Johnson, 2009). Even though the targeting of CDK2 does not have to be an optimal strategy for cancer treatment because of the redundancy of CDKs in cell cycle regulation (Tetsu and McCormick, 2003), the CDK2 has remained a paradigm for rational drug design, because it is the best characterized CDK in terms of structure and biochemistry (Echalier et al., 2010).

As the ATP-binding pocket is present in all kinases, it is usually the site targeted by kinase inhibitors. Although the structure of the ATP binding site is conserved between the kinases, there are subtle differences between them, enabling drugs to specifically target one subclass without affecting the others. Small molecule

* Corresponding author. Tel.: +91 4565 223342 650/365; fax: +91 4565 225202.
E-mail address: skysanjeev@gmail.com (S.K. Singh).

inhibitors competitively occupy the ATP binding pocket, often mimicking the hydrogen bonds made by the alanine moiety of ATP (Blagden and de Bono, 2005). Competition between an inhibitor and the native ATP substrate is an effective strategy to inhibit CDK2. An inhibitor binds to a deep cleft between two CDK2 lobes and, despite the numerous structurally varied CDK2 inhibitors known today, some common features can be identified. The discovery of the CDK2-inhibitor structure (De Azevedo et al., 1996, 1997) provided a useful starting point for the rational design of CDK2 inhibitors.

It is generally recognized that drug discovery and development are time and resource consuming process, requires various stages of screening. There is an ever growing effort to apply computational power to the combined chemical and biological space in order to streamline drug discovery, design, development and optimization (Kumar et al., 2006). Commonly used computational approaches include ligand-based and structure based drug design (Dror et al., 2004; Schneidman-Duhovny et al., 2004). An effective way to predict the binding of substrate with its receptor is docking simulation, which is successfully implemented in many applications (Dessalew and Singh, 2008; Otyepka et al., 2000; Vadivelan et al., 2007). Docking procedures basically aim to identify the correct conformation of ligands in the binding pocket of a protein and to predict the affinity between the ligand and protein (Dixon and Blaney, 1998). Several studies which provide independent benchmarks for widely used docking programs and among them the Glide was considered most accurate docking tools, which has been thoroughly reviewed in the literature over the years and has produced some notable successes (Perola et al., 2004; Friesner et al., 2004, Englebienne et al., 2007; Zhou et al., 2007). To test the molecular docking in this study, we selected Glide as they employ significantly different docking methodologies (Friesner et al.; 2004; Halgren et al., 2004; Friesner et al.; 2006) and have employed different collections of crystal complexes and binding data to weight their optimization algorithms.

The comparably fast and inexpensive docking protocols can be combined with accurate but more expensive molecular dynamics (MD) simulation techniques to predict more reliable protein–ligand complex structures (Karplus and McCammon, 2002; Norberg and Nilsson, 2003). On one hand docking techniques are used to search massive conformational space in a short time, allowing the analysis of a large library of drug compounds at a sensible cost (Kitchen et al., 2004). On another hand, MD simulation accounts for both ligand and protein in a flexible way, allowing for an induced fit into the receptor-binding site around the newly introduced ligand (Lin et al., 2002). MD simulation can be used: during the preparation of protein receptor before docking, to optimize its structure and account for protein flexibility (Schames et al., 2004); for the refinement of the docked complex, to include solvent effects and account for induced fit (Huo et al., 2002). This also calculates binding-free energies (Brandsdal et al., 2003), as well as providing an accurate ranking of the potential ligands (Wang et al., 1999).

In this work, we bring further information to understand the binding modes of known imidazo(1,2-*b*)pyridazines, 3,5-diaminoin-dazoles and triazolo(1,5-*a*) pyridazines series of CDK2 inhibitors using molecular docking, MD simulation and free-energy calculation. MD simulations were carried out to determine the stability and dynamical changes of predicted binding conformations. An MM-GB/SA (Molecular Mechanics-Generalized Born/Surface Area) analysis was carried out to calculate the binding free energies of the proteins with CDK2 inhibitors. We also examined in detail the role of H bonding with ligand. We show that the origin of selectivity with these inhibitors with key sites of the CDK2 contributing to the binding of these inhibitors. The information from this study will be highly useful to design or optimize CDK2 inhibitors by these molecular modeling approaches.

2. Materials and method

All computational analyses were carried out on Red Hat 5.1 Linux platform in IBM System x 3200 M2 server on Intel Xeon quad-core 2.83 GHz.

2.1. Biological data

Significantly, the biological activity of a compound against a receptor relies on its binding, which primarily depends on the structurally steric orientation and the electrostatic property. It is usual that small structure difference may give rise to a great biological diversity. Therefore, 27 compounds from 3,5-diaminoin-dazoles, imidazo(1,2-*b*)pyridazines, and triazolo(1,5-*a*)pyridazines series of CDK2 based on their wide range biological activity and structural diversity were taken from literature (Lee et al., 2008; Byth et al., 2004; Richardson et al., 2006). The structure of these inhibitors along with free energy of binding and their biological activity (pIC_{50} value) are shown in Table 1.

2.2. Preparation of protein target structure

In the present study, the X-ray crystal structure of CDK2 in complex with compound **14** (PDB ID: 1URW) was obtained from Protein Data Bank (Berman et al., 2000) and further prepared by protein preparation wizard, which is available in Glide (2011). The protein preparation wizard facility has two components namely, preparation and refinement. After ensuring chemical accuracy, the preparation component adds hydrogen and neutralizes side chain that is neither close to binding cavity nor involve in formation of salt bridges. OPLS-AA force field was used for this purpose and then active site of protein was defined. Glide uses full OPLS-AA force field at an intermediate docking stage and is claimed to be more sensitive to geometrical detail compare to other docking algorithms. In the next step, water molecules were removed and H atoms were added to structure, most likely positions of hydroxyl and thiol hydrogen atoms, protonation states and tautomers of His residue and Chi 'flip' assignment for Asn, Gln and His residue were selected by protein assignment script provided by Schrödinger. Minimization was performed until the average root mean square deviation of the nonhydrogen atoms reached 0.3 Å.

2.3. Ligand preparation

All the compounds were constructed using the fragment library of Maestro 9.2, and all compounds were prepared by using the LigPrep 2.4 (LigPrep, 2011), which can produce a number of structures from each input structure with various ionization states, tautomers, stereochemistries and ring conformations to eliminate molecules using various criteria including molecular weight or specified numbers and types of functional groups present with correct chiralities for each successfully processed input structure. The OPLS-2005 force field was used for optimization, which produces the low-energy conformer of the ligand (Hayes et al., 2004).

2.4. Molecular docking simulation

To test the docking parameters all compounds were docked into the binding site of the CDK2 protein (PDB ID: 1URW) using Grid-Based Ligand Docking With Energetics (Glide) software from Schrödinger (Halgren et al., 2004; Friesner et al., 2004). To soften the potential for nonpolar parts of the receptor, the scaling factor for protein van der Waals radii was 1.0 in the receptor grid

Table 1
Structure of compounds 1–27 along with their biological activity.

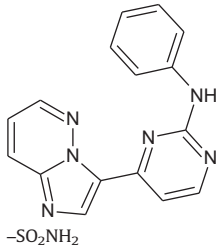
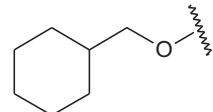
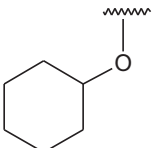
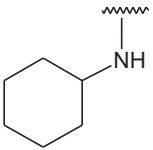
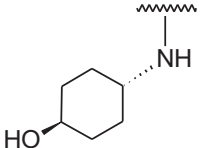
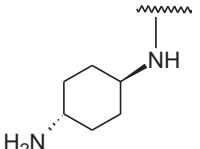
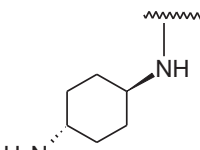
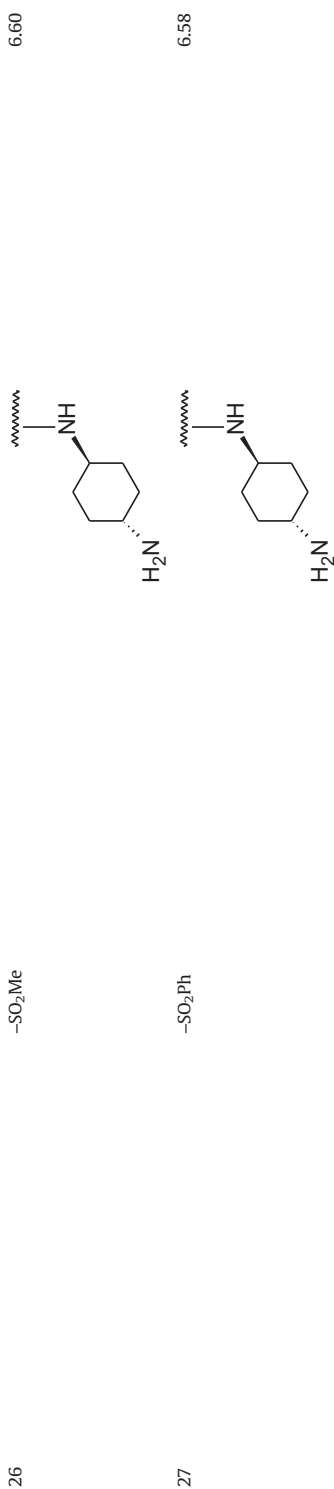
Compounds	R1	R2	pIC ₅₀ Values (μM)
1	NO ₂	–	5.69
2	C ₂ H ₅ NH	–	6.30
3	(C ₂ H ₅) ₂ N	–	6.69
4	(<i>n</i> -C ₃ H ₇) ₂ N	–	5.74
5	(<i>n</i> -C ₄ H ₉) ₂ N	–	4.00
6	CO(CH ₂) ₃ N	–	6.76
7	CO(CH ₂) ₄ N	–	5.14
8	COCH ₂ NHCON	–	5.69
9	SO ₂ (CH ₂) ₃ N	–	7.44
10	H	H	8.52
11	Me	H	8.52
12	(CH ₂) ₂ OMe	H	8.52
13	(CH ₂) ₂ NMe ₂	H	8.09
14	(CH ₂) ₃ NMe ₂	H	8.52
15	(CH ₂) ₂ OMe	Me	7.22
16	H	H	6.22
17	H	MeO	8.52
18	–	–	6.00
19	 -SO ₂ NH ₂		4.95

Table 1 (continued)

Compounds	R1	R2	pIC ₅₀ Values (μM)
20	-SO ₂ NH ₂		6.45
21	-SO ₂ NH ₂		6.13
22	-SO ₂ NH ₂		5.13
23	-SO ₂ NH ₂	Et ₂ N	6.39
24	-SO ₂ NH ₂		6.56
25	-SO ₂ NMe ₂		6.92



generation with a partial atomic charge of 0.25 i.e. Glide docking parameters were set to the default hard potential function. No constraints were applied for all the docking studies. A grid box with coordinates $X=10.869$, $Y=-9.290$, and $Z=9.489$ was generated at the centroid of the active site for docking. The active site was defined with a 10 Å radius around the ligand present in the crystal structure. The default grid size was adopted from the Glide program. The ligands were docked with the active site using the 'extra precision' glide docking (Glide XP) which docks ligands flexibly. Glide generates conformations internally and passes these through a series of filters. In XP docking, only active compounds will have available poses that avoid these penalties and also receive favorable scores for appropriate hydrophobic contact between the protein and the ligand, hydrogen-bonding interactions, and so on. The purposes of the XP method are to weed out false positives and to provide a better correlation between excellent poses and good scores (Friesner et al., 2006). The first places the ligand center at various grid positions of a 1 Å grid and rotates it around the three Euler angles. At this stage, crude score values and geometrical filters weed out unlikely binding modes. The next filter stage involves a grid-based force field evaluation and refinement of docking solutions, including torsional and rigid body movements of the ligand. The OPLS-2005 force field is used for this purpose. A small number of surviving docking solutions can then be subjected to a Monte Carlo procedure to try and minimize the energy score. The *maxkeep* variable which sets the maximum number of poses generated during the initial phase of the docking calculation were set to 5000 and the *keep best* variable which sets the number of poses per ligand that enters the energy minimization was set to 1000. Energy minimization protocol includes dielectric constant of 4.0 and 1000 steps of conjugate gradient. Upon completion of each docking calculation, at most 100 poses per ligand were generated. The final best docked structure was chosen using a Glidescore function, Glide energy and Glide Emodel energy. The Glidescore is a modified and extended version of the empirically base function (Eldridge et al., 1997), Glide energy is Modified Coulomb–van der Waals interaction energy and Glide Emodel, which combines glidescore, coulombic, van der waals and strain energy of the ligand. The lowest-energy docked complex was found in the majority of similar docking conformations. Finally, the lowest-energy docked complex was selected for further study.

2.5. Free energy calculation

The free energy of binding is calculated using Prime/MM-GB/SA approach. This approach is used to predict the free energy of binding for set of ligands to the receptor. The docked poses were minimized using the local optimization feature in Prime, and the energies of complex were calculated using the OPLS-AA (2005) force field and generalized-Born/surface area (GB/SA) continuum solvent model. The free energy of binding, ΔG_{bind} is calculated as (Lyne et al., 2006; Das et al., 2009):

$$\Delta G_{\text{bind}} = \Delta E + \Delta G_{\text{solv}} + \Delta G_{\text{SA}} \quad (1)$$

$$\Delta E = E_{\text{complex}} - E_{\text{protein}} - E_{\text{ligand}} \quad (2)$$

where E_{complex} , E_{protein} , and E_{ligand} are the minimized energies of the protein–inhibitor complex, protein, and inhibitor, respectively

$$\Delta G_{\text{solv}} = G_{\text{solv}(\text{complex})} - G_{\text{solv}(\text{protein})} - G_{\text{solv}(\text{ligand})} \quad (3)$$

where $G_{\text{solv}(\text{complex})}$, $G_{\text{solv}(\text{protein})}$, and $G_{\text{solv}(\text{ligand})}$ are the salvation free energies of the complex, protein, and inhibitor, respectively:

$$\Delta G_{\text{SA}} = G_{\text{SA}(\text{complex})} - G_{\text{SA}(\text{protein})} - G_{\text{SA}(\text{ligand})} \quad (4)$$

where $G_{SA(\text{complex})}$, $G_{SA(\text{protein})}$, and $G_{SA(\text{ligand})}$ are the surface area energies for the complex, protein and inhibitor, respectively.

The simulations were carried out using the GBSA continuum model (Koh et al., 2009) in Prime, version 2.2 (Prime, 2011). Prime uses a surface generalized Born (SGB) model employing a Gaussian surface instead of a van der Waals surface for better representation of the solvent-accessible surface area (Koh et al., 2009; Das et al., 2009).

2.6. Molecular dynamics simulation

2.6.1. System building

All molecular dynamics (MD) simulations were carried out on energy minimized CDK2-representative compound using the Desmond module of Schrodinger (Bowers et al., 2006a; Desmond, 2011). Desmond employs a particular neutral territory method (Shaw, 2005; Bowers et al., 2007) called the midpoint method (Bowers et al., 2006b) to efficiently exploit a high degree of computational parallelism. The OPLS-2005 force field (Jorgensen et al., 1996; Kaminski et al., 2001) was used in this system for protein interactions and solvated with the simple point charge (SPC) water model (Berendsen et al., 1981). The orthorhombic water box (volume CDK2=373277 Å³) allowing for a 10 Å buffer region between protein atoms and box sides. Overlapping water molecules were deleted and the systems neutralized with Na⁺ ions.

2.6.2. Simulation details

Force field parameters for the protein–ligand systems were assigned using the OPLS-AA (2005) force field (Jorgensen et al., 1996; Kaminski et al., 2001). ESP fit atomic partial charges from the DFT calculations on the ligands were used. Heavy atom bond lengths with hydrogens and the internal geometry of water molecules were constrained using the SHAKE algorithm (Ryckaert et al., 1977). Periodic boundary conditions (PBC) and a 9.0 Å cut-off for nonbond interactions were used, with electrostatic interactions treated using the Particle Mesh Ewald (PME) method (Essmann et al., 1995). A six relaxation protocol was employed prior to the MD production run: (i) 2000 steps LBFGS minimization (first 10 steps steepest descent algorithm) with the solute restrained and a loose convergence criteria of 50 kcal mol⁻¹ Å⁻¹; (ii) 2000 steps LBFGS minimization (first 10 steps steepest descent) with residues beyond 15 Å of ligands restrained and a convergence criteria of 5 kcal mol⁻¹ Å⁻¹; (iii) a short 12-ps simulation in the NVT ensemble using a temperature (T) of 10 K (thermostat relaxation constant=0.1 ps) with nonhydrogen solute atoms restrained; (iv) a 12-ps simulation in the NPT ensemble using T=10 K (thermostat relaxation constant=0.1 ps) and pressure (P)=1 atm (barostat relaxation constant=50 ps) with nonhydrogen solute atoms restrained; (v) a 24 ps simulation in the NPT ensemble (T=300 K; thermostat relaxation constant 0.1 ps; P=1 atm; barostat relaxation constant 50.0 ps) with solute nonhydrogen atoms restrained; and (vi) a 24-ps simulation in the NPT ensemble (T=300 K; thermostat relaxation constant 0.1 ps; P=1 atm; barostat relaxation constant 2.0 ps) with residues beyond 15 Å of the ligands restrained. For all of the above atomic restraints, a 50 kcal mol⁻¹ Å⁻² restraint force constant was used, while target temperatures and pressures were controlled using Berendsen thermostats and barostats, respectively (Berendsen et al., 1984). For the dynamics, a multiple time step RESPA integration algorithm was used throughout with time steps of 2, 2, and 6 fs for bonded, ‘near’ nonbonded, and ‘far’ nonbonded interactions respectively. Following the relaxation, a 5 ns MD run in the NPT ensemble (T=300 K, thermostat relaxation time=1.0 ps; P=1 atm; barostat relaxation time=2.0 ps) was performed for each system using a Nose–Hoover thermostat and Martyna–Tobias–Klein

barostat (Martyna et al., 1992; Martyna et al., 1994). Energy and trajectory atomic coordinate data were recorded at every 1.2 and 5.0 ps, respectively. 3-D structures and trajectories were visually inspected using the Maestro graphical interface. Root mean square deviations (RMSDs) from the initial structures were calculated using superposition option in Maestro. An average structure obtained from the last 250 ps of MD simulations was refined by means of 1000 steps of steepest descent followed by conjugate gradient energy minimization. The maximum number of cycle of minimization was 5000 and the convergence criterion for the energy gradient was 0.001 kJ/mol Å.

3. Results and discussion

3.1. Analysis of binding site of CDK2 protein

The ATP-binding site of CDK2 has significant hydrophobic region and several key sites of interest for the design of CDK2 inhibitors. The CDK2 protein has a bilobal shape formed by the association of a N-terminal domain rich in beta-sheets (small lobe) and a C-terminal domain constituted of helices (large lobe). The smaller N-terminal lobe of CDK2 consists of a sheet of antiparallel β -strands (β 1– β 5) and a single large helix (α 1). The larger C-terminal lobe contains a pseudo-4-helical bundle (α 2, 3, 4, 6), a small β -ribbon (β 6– β 8), and two additional helices (α 5, 7). The binding site of the ATP is a cleft located at the interface of the two domains. This cleft can be divided into three regions defined by the reference to the chemical moieties in ATP. The first one of the hydrophobic characters comprises amino acids Ile10, Ala31, Val64, Phe80, Glu81, Phe82, Leu83, Leu134 and Ala144 and forms the environment of the adenine moiety of ATP as shown in Fig. 1 (De Bondt et al., 1993; Furet, 2003).

More precisely, the adenine ring is ‘‘sandwiched’’ between Ala31 and Leu134 with which it makes close hydrophobic contacts. In addition, its N6 and N1 atoms form hydrogen bonds, in a bidentate manner, with the backbone carbonyl of Glu81 and the backbone NH of Leu83, respectively. These residues belong to the amino acid stretch that connects the two domains of the kinase, the so called hinge segment (De Bondt et al., 1993; Furet, 2003). The second region corresponds to the three amino acids that interact with the ribose moiety of ATP. Val18 of the glycine-rich loop is in van der Waals contact with the ring while Asp86 and Gln131 make hydrogen bonds with its hydroxyl substituents. Finally, polar amino acids fixing the conformation of the triphosphate chain of ATP, either by direct interaction with Lys33 or by mediation of a magnesium cation interaction with Asp145 and Asn132, constitute the third region. The molecular superposition of bound conformations of representative compounds from each series indicates that these compounds have more or less identical binding mode with CDK2, especially for the hinge interaction site region and the phosphate binding region (Fig. 2).

The structural analysis described above suggests that the hydrophobic character amino acids, amino acids that interact with the ribose moiety of ATP and polar amino acids fixing the conformation region could be exploited to improve the pharmacokinetic properties of lead compounds against CDK2.

3.2. Validation of the docking protocol

The most significant method of evaluating the accuracy of a docking procedure is to determine how closely the lowest energy poses (binding conformation) predicted by the object scoring function, Glidescore (Gscore or docking score) in the present study, almost resembles an experimental binding mode as determined X-ray crystallography (Talele and McLaughlin, 2008). In the

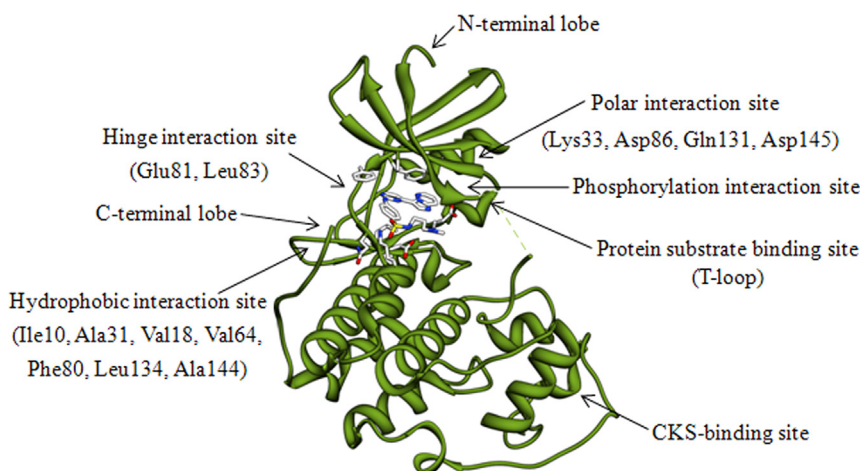


Fig. 1. Architecture of the CDK2 different binding sites and compound **14** bound to ATP binding site of CDK2 (PDB ID: 1URW). Protein backbone atoms are depicted by ribbons.

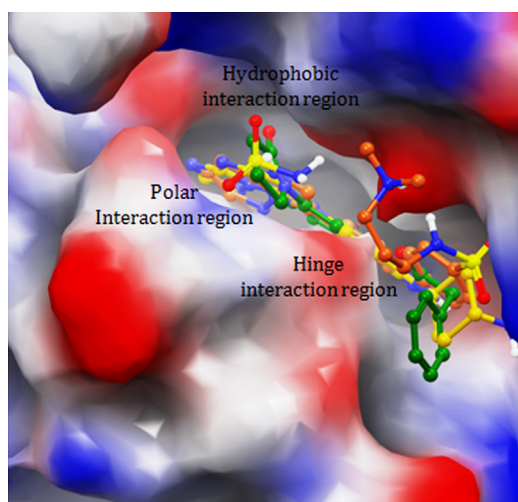


Fig. 2. Extra precision (XP) docking predicted pose for representative compounds from each series: compounds **6** (green), **14** (yellow) and **24** (orange) resulting from molecular docking and their superposition in the ATP-binding site of CDK2. CDK2 is represented as surface according to residue charge (electropositive charge: blue, electronegative charge: red, neutral: white). (For interpretation of the references to color in this figure caption, the reader is referred to the web version of this article.)

present study, extra precision (XP) Glide docking procedure was validated by removing the compound **14** from the binding site and redocking it to the binding site of CDK2 (PDB ID: 1URW). We found very good interaction between the localization of the inhibitor upon docking and from the crystal structure of CDK2 (PDB ID: 1URW), i.e. having almost similar hydrogen bonding interactions with Leu83, and with Asp86. Interestingly, our Glide XP docking mode also exposed additional π - π stacking with Phe80, which is an attractive, noncovalent interaction between aromatic rings (McGaughey et al., 1998; Sinnokrot et al., 2002). The root mean square deviation (RMSD) between the predicted conformation and the observed X-ray crystallographic conformation of the compound **14** (PDB ID: 1URW) equal to 0.50 Å (Fig.3d), a value that suggest the reliability of Glide XP docking mode in reproducing the experimentally observed binding mode for CDK2 inhibitors and the parameter set for Glide XP docking is reasonable to reproduce the X-ray structure (Table 2).

Docking experiments were further performed with crystal structures of CDK2 including 1E1V and 3NS9. Comparison of the docked pose and the crystallographic mode was performed for both structures. The RMSD values between the docked pose and its bound

conformation for 1E1V and 3NS9 are 0.69 and 0.91 Å, respectively. Additionally, considering that different inhibitors induce different conformational changes, Glide docking was also performed with crystal ligand of 1E1V and 3NS9 in the active site of 1URW and docked pose further superimposed with original crystal of 1E1V and 3NS9 of CDK2. The RMSD values between the docked pose and its bound conformation for 1E1V and 3NS9 are 0.73 and 0.82 Å, respectively, thus indicating that Glide docking performed well for CDK2. This signifies that the PDB structure 1URW is a typical structure to perform docking studies on different compounds to yield reasonable accuracy. This is one of the reasons to attain a good correlation between biological activity and free energy of binding for different ligands. The top views of the docked poses of the ligands and their bound conformations in the crystal structures are illustrated in Figs. S1 and S2 of Supplementary material. It has been observed that the RMSD value between the crystal and predicted conformation is widely used as an indicator of whether correct docking pose was obtained by the program or not (Kroemer et al., 2004). Usually, an RMSD of 2 Å is considered as the cutoff of correct docking, probably because the resolution in an X-ray crystal structure analysis is often about 2 Å, and higher precision than the resolution of the analysis is not meaningful (Onodera et al., 2007). After this validation, all of the 27 inhibitors of CDK2 in the data set were docked into the X-ray crystallographic structure of CDK2 (PDB ID: 1URW).

3.3. Extra precision docking studies

A group of 27 known compound from 3,5-diaminoindazoles, imidazo(1,2-*b*)pyridazines, and triazolo(1,5-*a*) pyridazines series of CDK2 inhibitors were selected from literature (Lee et al., 2008; Byth et al., 2004; Richardson et al., 2006) to investigate their binding mode within the binding site of CDK2. Glide XP docking was carried out and in each XP docking maximum of 100 poses were saved. After the graphical analysis of the CDK2, the same relative orientation for each compound was selected. The predicted binding affinity, energy of best docked compound, Emodel energy and their key interaction in the active site are shown in Table 2. On the basis of the nature of amino acid and their interaction with different series of compounds, these compounds can be grouped into hinge interactions, hydrophobic interactions and polar interactions.

3.3.1. Binding mode of 3,5-diaminoindazoles, imidazo(1,2-*b*)pyridazines, and triazolo(1,5-*a*)pyridazines series of CDK2 inhibitors

A comparison of the different XP Glide docking poses of compounds **1–27** from 3,5-diaminoindazoles, imidazo(1,2-*b*)

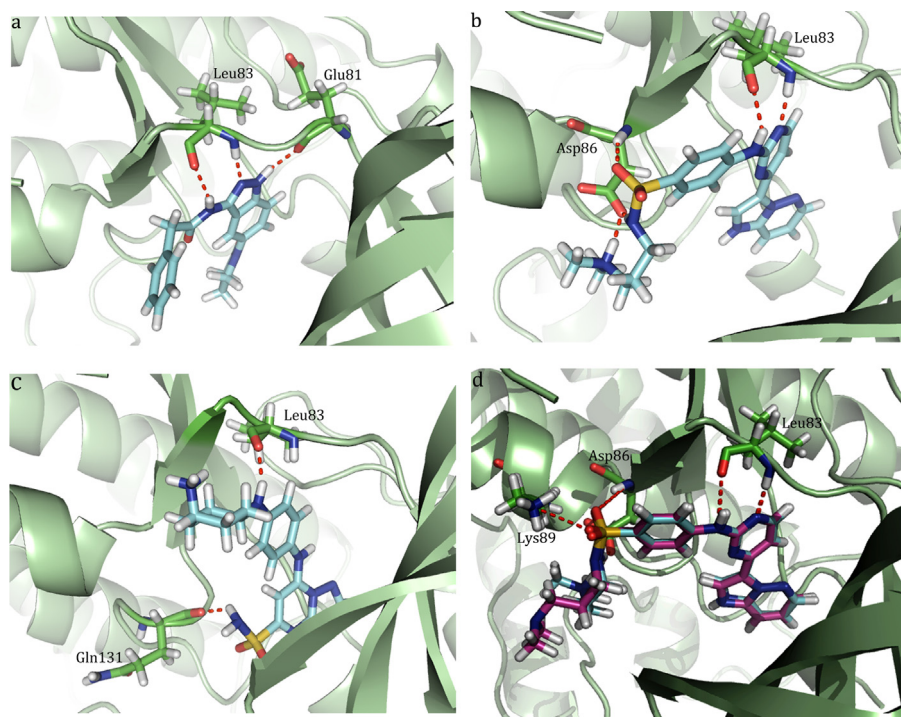


Fig. 3. Extra precision Glide docking (1URW) with (a) compound **6**, (b) compound **14** (c) compound **24**, showing hydrogen bond with interaction amino acids, (d) Overlay of docked pose (cyan) of compound **14** with its crystal structure conformation (pink). (For interpretation of the references to color in this figure caption, the reader is referred to the web version of this article.)

Table 2

Extra precision Glide docking results with interacting amino acids in the active of CDK2.

Compounds	Glide XP Docking Score	Glide XP energy (kcal/mol)	Glide XP Emodel (kcal/mol)	Interacting amino acids	HB ^b	RMSD (Å)
1	-9.95	-50.19	-66.94	Glu81, Leu83(2) ^a	3	0.44
2	-10.69	-58.41	-66.00	Glu81, Leu83(2) ^a	3	0.25
3	-11.18	-59.80	-79.88	Leu83(2) ^a	2	0.29
4	-11.42	-53.78	-82.01	Leu83(2) ^a	2	0.35
5	-11.49	-67.14	-87.45	Glu81, Leu83(2) ^a	3	0.33
6	-11.78	-69.65	-98.80	Glu81, Leu83(2) ^a	3	0.43
7	-10.01	-67.87	-71.56	Leu83(2) ^a	2	0.46
8	-11.44	-65.01	-89.68	Leu83(2) ^a	2	0.20
9	-10.87	-56.92	-69.68	Leu83(2) ^a	2	0.40
10	-13.49	-69.11	-95.24	Leu83(2) ^a , Asp86(2) ^a	4	0.40
11	-13.47	-77.15	-104.29	Leu83(2) ^a , Asp86(2) ^a	4	0.44
12	-13.46	-67.52	-91.47	Leu83(2) ^a , Asp86(2) ^a	4	0.23
13	-14.56	-82.46	-119.45	Leu83(2) ^a , Asp86(3) ^a	5	0.45
14	-14.50	-85.03	-112.79	Leu83(2) ^a , Asp86(3) ^a	5	0.50
15	-11.26	-65.04	-79.69	Leu83(2) ^a , Asp86, Lys89	4	0.18
16	-12.71	-58.98	-108.78	Leu83(2) ^a , Asp86(3) ^a	5	0.37
17	-13.51	-70.70	-107.77	Leu83(2) ^a , Asp86(2) ^a	4	0.10
18	-10.60	-48.47	-69.18	Leu83(2) ^a	2	0.28
19	-4.84	-59.10	-68.92	Gln131	1	0.18
20	-7.71	-43.07	-79.17	Gln131	1	0.60
21	-7.22	-42.66	-61.22	Gln131	1	0.31
22	-7.48	-47.80	-87.79	Leu83, Gln131	2	0.35
23	-7.73	-44.57	-69.97	Leu83, Gln131	2	0.50
24	-6.99	-51.40	-69.56	Leu83, Gln131	2	0.80
25	-6.82	-48.62	-66.86	Leu83, Gln131	2	0.71
26	-5.26	-58.06	-63.44	Leu83, Gln131	2	0.26
27	-6.01	-48.03	-77.55	Leu83	1	0.71

^a Forms two or more than two hydrogen bond interaction in same amino acid residue.

^b Number of hydrogen bonds formed.

pyridazines, and triazolo(1,5-*a*) pyridazines series of CDK2 inhibitors respectively suggests that these compounds adopt similar binding modes with the H-bonding network. To illustrate the binding mode of this series of compounds, compound **6**, **14** and **24** from each series of CDK2 inhibitors, was analyzed in more detail.

Fig. 3a–c shows a binding mode of compound **6**, **14**, and **24** into the active site of CDK2, in which compound **14** has previously crystal bound structure with active site of CDK2 (PDB ID: 1URW) and explained in more detail in validation of the docking protocol section. The geometric criteria (distance and angle) have been

used as default to define a hydrogen bond. Glide sets these values internally, to H-acceptor maximum distances of 2.5 Å; minimum donor angle of 120°, and minimum acceptor angle of 90°.

A comparison of different docking poses from 3,5-diaminoin-dazoles series (compound **1–9**) are showing hydrogen bonding network with Glu81 and Leu83 and these residues belongs to the amino acid stretch that connects the two domains of the kinase, the so called hinge segment. To illustrate the binding mode of this series, compound **6** was selected for more detailed analysis. Fig. 3a shows the docked model of compound **6** within the active site of CDK2. Interaction with the hinge segment is remarkably conserved in all crystal structures (Furet, 2003). With the result all compound from 3,5-diaminoin-dazoles series in Table 2, form at least two direct hydrogen bond with the hinge segment. Precisely, they all accept a hydrogen bond from the backbone NH and C=O ($rNH \cdots N$ and $rC=O \cdots HN$) of Leu83. Even more closely mimicking ATP, some inhibitors (De Azevedo et al., 1996; Mani et al., 2000; Legraverend et al., 2000) form a second hydrogen bond with the backbone carbonyl ($rC=O \cdots HN$) of Glu81. However, more often, the second hydrogen bond engages the backbone carbonyl of the same residue Leu83 (Morgan, 1997; Rosania and Chang, 2000). Another interesting observation is that the natural inhibitor p27 also utilizes hydrogen bonds to the backbone of Leu83 and Glu81 to block the ATP binding site of CDK2 by insertion of a tyrosine residue in the pocket (Russo et al., 1996). Thus, the chemical inhibitors can also be viewed as mimics of the natural inhibitor of CDK2.

A comparison of different docking poses from imidazo(1,2-*b*) pyridazines series (compounds **10–18**) are showing hydrogen bonding network with Leu83 (hinge segment), Asp86 and Lys89, residues belongs to polar interaction site. To illustrate the binding mode of this series, compound **14** was selected for more detailed analysis. Fig. 3b shows the docked model of compound **14** within the active site of CDK2. Precisely, they all accept a hydrogen bond from the backbone NH and C=O ($rNH \cdots N$ and $rC=O \cdots HN$) of Leu83, second hydrogen bond with the backbone NH and C=O ($rNH \cdots O=S$, $rC=O \cdots HN$ and $rC=O \cdots HN$) of Asp86. The Asp86 is one of the important amino acids of the ribose moiety of ATP, which make hydrogen bonds with its hydroxyl substituents. Finally, polar amino acids fixing the conformation of the triphosphate chain of ATP, either by direct interaction or by mediation of a magnesium cation. Asp86 of the ribose region are also used by the inhibitors for binding to the pocket (Furet, 2003). Remarkably, all the inhibitors containing a sulfonamide or sulfone group present a hydrogen bond between one of the oxygen atoms of this group and the backbone NH of Asp86 (Clare et al., 2001; Furet et al., 2001).

A comparison of different docking poses from triazolo(1,5-*a*) pyridazines series (compounds **19–27**) are showing hydrogen bonding network with Leu83 (hinge segment) and Gln131 residue belongs to polar interaction site. To illustrate the binding mode of this series, compound **24** was selected for more detailed analysis. Fig. 3c shows the docked model of compound **24** within the active site of CDK2. Precisely, they all accept a hydrogen bond from the backbone C=O ($rC=O \cdots HN$) of Leu83, second hydrogen bond through its backbone carbonyl ($rC=O \cdots HN$) of Glu131. Out of three amino acids, Gln131 is also one of the important amino acids that interact with the ribose moiety of ATP. Val18 of the glycine-rich loop is in van der Waals contact with the ring while Asp86 and Gln131 make hydrogen bonds with its hydroxyl substituents. Finally, polar amino acids fixing the conformation of the triphosphate chain of ATP, either by direct interaction or by mediation of a magnesium cation. Gln131 of the ribose region is also used by the inhibitors for binding to the pocket. Gln131 is seen to interact through its backbone carbonyl with the amine function on the tetrahydropyran ring of staurosporine (Legraverend et al., 2000)

and through its side chain with the hydroxyethylamino group of olomoucine (Rosania and Chang, 2000).

Interestingly, our Glide XP docking mode also exposed additional π - π stacking with Phe80 (Fig. 4b and c), which is an attractive, noncovalent interactions between aromatic rings, which also play an important role in stabilization of drug in active site (Fig. 4a–c) (Sinnokrot et al., 2002). The Phe80 is one of the key amino acids of hydrophobic interaction site, which is composed of Ile10, Ala31, Val64, Phe80, Glu81, Phe82, Leu83, Leu134 and Ala144 and forms the environment of the adenine moiety of ATP. The latter residues only weakly interact with ATP (intermolecular atomic distances greater than 4 Å). Thus, it appears that the additional hydrophobic interactions with these residues are largely responsible for the high binding affinity that most inhibitors display compared to ATP. Moreover, Glide XP-scores (GScore) showed statistically fair correlation coefficient of 0.57 and 0.59 with Glide energy and Glide emodel, respectively (Fig. 5).

There are some theoretical and experimental data that support our findings about the significance of hydrogen bond interactions in this protein–ligand system. For instance, Alzate-Morales et al. (2009) mainly focused on the study of the hydrogen bond interactions between hinge region (typical triplet of hydrogen bond interactions with Glu81 and Leu83) and some residues at the solvent channel for rank the set of CDK2 inhibitors. Tripathi et al. (2012) found that Leu83 is a key residue that recognizes BS194 more effectively with CDK2 with good binding free energies rather than CDK1. Aixiao et al. (2008) found that residues Asp86, Leu83, Lys33, and Lys89 are important in determining the selectivity of compound 2PU by CDK2 or CDK4 enzymes. Some additional experimental findings support the essential role of the hydrogen bonds in the hinge region as well as the role of the residues Asp86 and Lys89 in the improved selectivity showed by some CDK2 inhibitors (Davies et al., 2002a; Griffin et al., 2006).

3.4. Binding free energy analysis

In the present work the evaluation of molecular docking with a related post-scoring approach, MM-GBSA is reported for CDK2. The results from free energy of binding prediction using MM-GBSA are listed in Table 3. Although more computationally demanding, the MM-GBSA scoring usually yields for significant correlation with experimentally determined activity (Lyne et al., 2006). The structural information of CDK2 has been key in driving the design and development of a diverse number of ATP competitive inhibitors. Crystallography has revealed that the ATP-binding site of CDK2 can accommodate a number of diverse molecular frameworks, exploiting various sites of interaction. In addition, residues outside the main ATP-binding cleft have been identified that could be targeted to increase specificity and potency. These results suggest that it may be possible to design pharmacologically relevant ligands that act as specific and potent inhibitors of CDK activity (Davies et al., 2002b, Furet, 2003). So far, 11 classes of CDK ATP competitive inhibitors have been developed: Staurosporine, Flavonoid, Purine, Indole, Pyrine, Pyrimidine, Indirubin, Pyrazole, Thiazole, Paullone and Hymenialdisine derivatives (Canavese et al., 2012). Structural feedback in the rational design of CDK inhibitors has been derived in the main from studies of monomeric CDK2/inhibitor complexes. These structures have shown that a large number of diverse compounds have the necessary ability to satisfy the hydrogen-bonding potential of the kinase hinge region (Leu83 and Glu81) in addition to complementing the shape and chemistry of the cleft. These diverse backbones provide frameworks for the development of future inhibitors through exploitation of subsites both within and outside the main binding cleft (Davies et al., 2002).

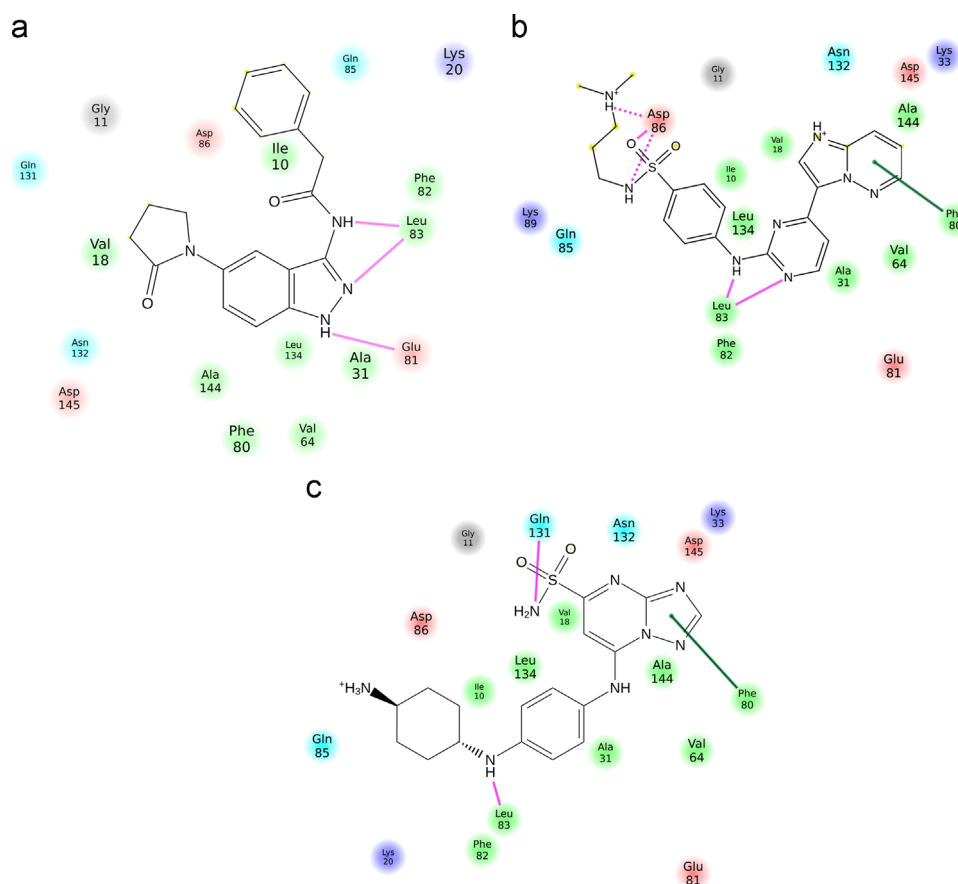


Fig. 4. 2D interaction map of important amino acids with Glide XP docking (1URW) for (a) Compound **6**, (b) compound **14**, (c) compound **24**, showing hydrogen bond interaction including π - π stacking.

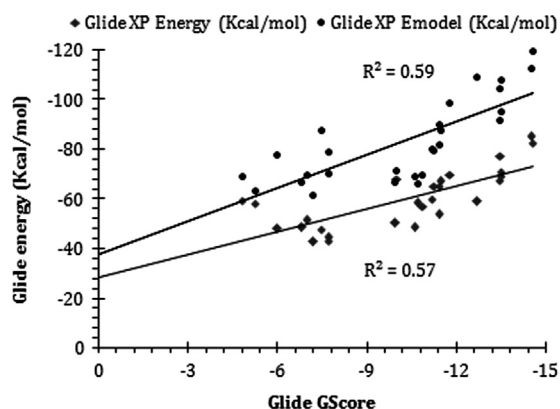


Fig. 5. Correlation of extra precision Glide docking score with glide energy and with glide emodel energy.

The different classes of CDK2 inhibitors were chosen to examine the ability of the approach to correctly rank the relative potencies of inhibitors against CDK2. The calculated binding energies are plotted against pIC_{50} for CDK2. As can be seen, the approach has been very successful at getting the correct relative rankings and there is a satisfactory correlation observed between the calculated and biological activity values in Fig. 6. The calculated free energies of the CDK2 complex with different series of inhibitors range from -47.99 to -92.40 kcal/mol ($\Delta G_{\text{bind}} = -47.29$ kcal/mol to -92.40 kcal/mol). According to the energy components of the binding free energies (Table 3), the major favorable contributors to ligand binding are van der Waals and Nonpolar solvation terms (ΔG_{solvSA}) whereas polar solvation (ΔG_{solvGB})

opposes binding. In all the active compounds Coulomb energy term disfavors the binding energy except the compound **13** which has strong Coulomb energy term. In all the active compounds the ΔG_{solvSA} was very strong and having the value > 50 kcal/mol but in most of the inactive compounds ΔG_{solvSA} is very less compared to highly active compound. Hence, it is clearly evident that ΔG_{solvSA} is the driving force for ligand binding.

We compare our results from this to those of Lyne et al. (2006) (in which the compounds were docked by Glide, and the best poses were scored using the same MM-GBSA force field employed here. Inhibitors of CDK2 were used as test set out of four kinases in that study. For CDK2, our results of $R^2 = 0.86$ is better than those reported by Lyne ($R^2 = 0.71$ for CDK2). In another study, for CDK2, our results of $R^2 = 0.86$ is also better than those reported by Rapp et al. (2011) ($R^2 = 0.82$ for CDK2). The correlation between the MM-GBSA results and biological activity data with diverse set is remarkable, and could be a more attractive alternative for rank-ordering than the Free Energy Perturbation (FEP) and Thermodynamic Integration (TI) methodologies because, while as accurate, it can handle more structurally dissimilar ligands and provides results at a fraction of the computational cost (Guimarães and Cardozo, 2008). As shown above (Table 2), Leu83 is frequent amino acid which is interaction with different series of inhibitors and the amine group plays an important role in recognition by CDK2.

3.5. Molecular dynamics simulation studies

To take into account protein flexibility, the behavior of the predicted complex was studied in a molecular dynamic simulations context for compounds **6**, **14** and **24** bound CDK2 in explicit aqueous solution were run for 5 ns. This MD simulation could

Table 3
Binding free energy calculation results for the different series of compound bound with CDK2.^a

Compound	ΔE			ΔG_{solv}	ΔG_{SA}	ΔG
	$\Delta G_{\text{Coulomb}}^b$	ΔG_{vdW}^c	$\Delta G_{\text{Covalent}}^d$			
1	-7.34	-39.42	7.04	3.76	-27.35	-63.31
2	-21.07	-40.62	2.21	20.50	-30.69	-69.67
3	-11.33	-46.02	1.69	18.44	-33.82	-71.04
4	-10.95	-47.55	2.72	19.26	-24.74	-61.26
5	-23.72	-42.47	12.46	23.39	-17.66	-47.99
6	-21.52	-45.23	2.98	20.52	-37.24	-80.49
7	-11.24	-50.15	1.95	20.14	-31.18	-70.48
8	-11.67	-50.09	3.80	17.94	-21.64	-61.66
9	16.00	-48.93	1.42	9.30	-57.81	-80.02
10	18.64	-53.67	1.35	19.11	-67.77	-84.34
11	12.25	-55.37	1.45	15.18	-61.86	-88.35
12	17.71	-58.61	1.32	16.65	-67.12	-90.05
13	-38.22	-53.01	2.30	46.81	-50.28	-92.40
14	17.67	-61.46	2.21	16.99	-62.70	-87.29
15	12.05	-60.30	2.27	10.80	-39.60	-74.78
16	7.60	-58.95	5.39	8.98	-27.02	-64.00
17	9.77	-57.40	3.66	12.34	-59.67	-91.30
18	-15.07	-46.94	9.66	14.51	-30.43	-68.27
19	25.90	-40.15	3.76	12.63	-54.08	-51.94
20	11.62	-27.84	2.71	8.05	-48.74	-54.20
21	-38.24	-40.55	12.77	20.81	-20.13	-65.34
22	15.08	-40.75	3.89	9.67	-46.81	-58.92
23	10.65	-18.00	2.90	6.77	-61.66	-59.34
24	-55.34	-40.46	11.80	41.79	-22.63	-64.84
25	-55.34	-47.15	14.96	37.05	-21.56	-72.04
26	16.32	-42.47	5.92	1.88	-49.45	-67.80
27	-38.82	-40.86	17.77	20.57	-24.20	-65.54

^a All energies are in kcal/mol.

^b Contribution to the free energy of binding from the Coulomb energy.

^c Contribution to the free energy of binding from the van der Waals energy.

^d Contribution to the free energy of binding from the covalent energy (internal energy).

^e Contribution to the free energy of binding from the generalized born electrostatic solvation energy.

^f Contribution to the free energy of binding from the surface area due to lipophilic energy (nonpolar contribution estimated by solvent accessible surface area).

^g Free energy of binding.

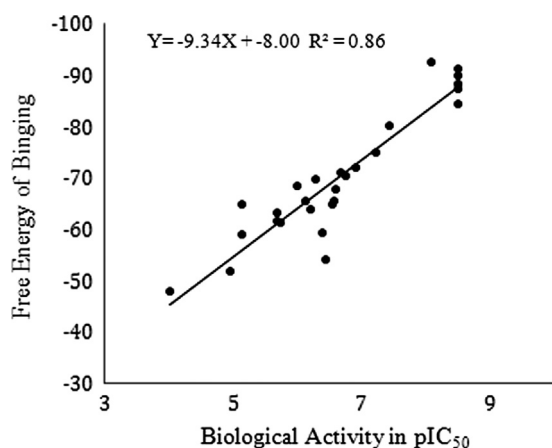


Fig. 6. Correlation between experimental pIC_{50} against CDK2 and calculated free energy of binding (kcal/mol) obtained by MM-GBSA.

be run for long duration to get more insight against predicted conformation. Even though, there are several studies for short duration MD simulation to get insight against predicted conformation (Jiang et al., 2005; Aixiao et al., 2008). To explore the dynamic stability of both systems and to ensure the rationality of the sampling method, RMSD from the starting structure are analyzed (Fig. 7a and b). The superposition of coordinates of each complex structure in a trajectory (250 structures) onto the initial structure

allowed us to analyze the progression of the root mean square deviations. The superposition of the coordinates of energy minimized average structure of compounds **6**, **14** and **24**/CDK2 complex obtained from the last 250 trajectories onto their respective starting complex provided RMSD of 0.897 Å, 0.683 Å and 1.068 Å, respectively for ligand atom-based superposition. Furthermore, the stability of the hydrogen bonding network predicted by Glide XP docking method was examined by monitoring the percentage occurrence of predicted hydrogen bonds during the simulation time. The analyses of the MD trajectories of representative inhibitors indicate the presence of several hydrogen bonds between the inhibitors and CDK2 with modest to high frequencies.

Based on Glide XP docking simulations, three hydrogen bonds were predicted for the compound **6**/CDK2 complex. Among these hydrogen bonds (Glu81 C=O...N, Leu83 C=O...HN and Leu83 NH...N), two were preserved in approximately 90% of the MD trajectory. The NH...N of Leu83 hydrogen bond appeared only in 20% of the trajectory. Among the five hydrogen bonds (Leu83 C=O...HN, Leu83 NH...N; Asp86 NH...O=S, Asp86 C=O...HN, Asp86 C=O...HN) in the compound **14**/CDK2 complex, only four were preserved in 75% of the MD trajectory. The Asp86 NH...O=S hydrogen bond appeared only in ~15% of the trajectory.

Relatively low frequency of Asp86 NH...O=S hydrogen bond is due to the fact that Asp86 side chain evolved through significant conformational flexibility as evident from the transient hydrogen bonding interaction between the imidazo(1,2-*b*)pyridazines and Asp86 side chain NH₂. All of the two hydrogen bonds (Leu83 C=O...HN, Gln131 C=O...HN) between the compound **24** and CDK2 were found to be stable during the simulation time. Leu83 was significantly preserved while remaining one (Gln131) was preserved only for approximately ~25% of the simulation time.

All the predicted hydrogen bonds (compound **6**, **14** and **24**/CDK2 complex) were restored in energy minimized average complex structure and it should be noted that those atoms which lost the hydrogen bonding interaction during MD simulations could still be involved in electrostatic interactions. The results of MD simulation of compound **6**, **14** and **24** with CDK2 complex are graphically shown in Fig. 7a and b. Most of the hydrogen bonds detected during MD simulations were formed with amino acid residues located within the hinge region and such hydrogen bonds probably reflect the high conformational freedom of amino acids near the hinge region than that of amino acids buried into the surface region.

In order to examine the sizes of bound compounds **6**, **14** and **24** with CDK2, their gyration radii (R_g) are estimated as shown in Fig. 7c, where R_g is known to be a parameter of molecular size. The gyration radius of each complex keeps stable after 2 ns MD simulation. The average values of compounds **6**, **14** and **24** complex are 19.50 Å, 19.56 Å and 19.84 Å, while the standard deviations are 0.129, 0.092 and 0.134, respectively. Thus, the similar shape and size of complexed CDK2 suggest that the structures of all complexes are stable. The descriptive analyses of RMSD of the compounds in 5 ns MD simulation from the initial structures are reported in Table 4. The maximum RMSD fitted to the starting structure of the compounds in the CDK2 complex is 1.48 Å, 1.84 Å and 1.53 Å. Moreover, the standard deviations for compound **6**, **14** and **24** complex with CDK2 are 0.153, 0.257 and 0.229, with confidence level (95.0%) of 0.004, 0.008 and 0.007, respectively. Fig. 7d shows the average means RMSD using bars, and the corresponding standard deviations are shown using error bars for compound **6**, **14** and **24** complex, respectively (Table 4).

3.6. Structure-based strategies to design new inhibitors against CDK2

The X-ray crystallography is most of the time simply used as an investigative tool that helps to rationalize the inhibitory activity of

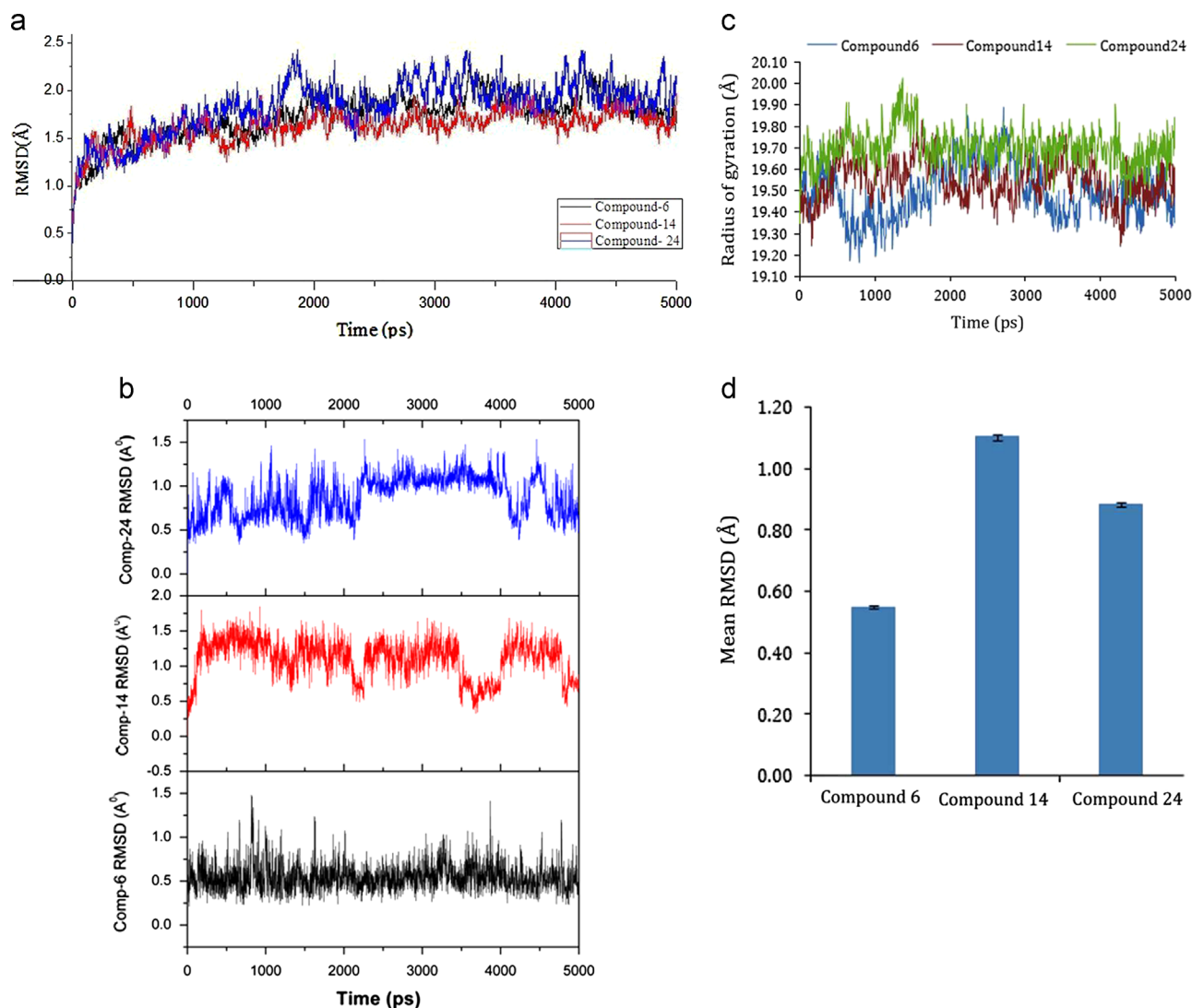


Fig. 7. The RMSD of backbone atoms of the protein (a) and the heavy atoms in the ligand (b) time dependences of gyration radii for bound CDK2 (c) the average means RMSD using bars, and the corresponding standard deviations are shown using error bars (d) for the compounds **6**, **14** and **24** bound CDK2 systems as a function of the simulation time.

Table 4

Descriptive analyses of RMSD of the compounds in 5 ns MD simulation.

Complex	Mean	Standard error	Median	Standard deviation	Minimum	Maximum	Confidence level (95.0%)
Compound 6	0.55	0.002	0.53	0.153	1.40	1.48	0.004
Compound 14	1.11	0.004	1.15	0.275	1.35	1.84	0.008
Compound 24	0.89	0.003	0.93	0.229	1.30	1.53	0.007

a compound identified by screening or some other approach. Even though the early availability of CDK2 crystal structures, relatively few reports of real exploitation of this information to optimize or design inhibitors have appeared in the literature (Furet, 2003). At various pharmaceutical companies, structure-based design is one of the main approaches for lead discovery in the protein kinase projects (Furet et al., 2001). In the present study, Glide XP docking results provide a better understanding of the active site regions in CDK2 that could be exploited as drug design targets. The presence of indazoles from 3,5-diaminoindazoles series (compounds **1–9**) showed dependency on the substituent at position 3 and 5, which is showing interaction in hinge region and polar interaction site of CDK2. The phenylacetyl type of substituents at position 5 can show

better inhibitory activity and to improve the pharmacokinetic profile of this class of compounds against CDK2. The imidazo (1,2-*b*)pyridazines (compounds **10–18**) series of compound showed a significantly greater dependence on the presence of sulfonamide substituents (SO₂NH). The sulfonamide group forms hydrogen bonds with the Asp86 backbone NH and its carboxylic side chain and also side chain NH of Lys89. The triazolo(1,5-*a*)pyridazines series (compounds **19–27**) of CDK2 inhibitors shows that the nitrogen of sulfonamide packs against the backbone of Gln131, showing relatively hydrophobic surface area. Even as the binding modes for the core and the sulfonamide moieties are conserved, the cyclohexyl group shows some differences in orientation between the different structures, which suggested that linker between the

triazolo(1,5-*a*)pyridazines core and the cyclohexyl group was flexible, and that the cyclohexyl moiety could make the favorable interactions with a number of residues in the active site of CDK2.

Our strategy consists of the interactive modeling design of molecular fragments that form the essential hydrogen bonds with the hinge segment and make favorable contacts with the hydrophobic residues of the adenine binding region of ATP. The different docking poses from 3,5-diaminoindazoles series, imidazo(1,2-*b*)pyridazines series and triazolo(1,5-*a*)pyridazines series is showing interesting observation of hydrogen bonding network with Glu81, Leu83, Asp86, Lys89 and Gln131, which block the ATP binding site of CDK2 (Furet, 2003). Furthermore, our understanding with full atomic details regarding ATP binding pocket of CDK2 could be exploited in medicinal chemistry for the design and optimization of CDK inhibitors. Judging from the successes already reported, the structure-based approach, by its efficiency and elegance, should become the method of choice for the discovery of new inhibitors in this important area of anti-cancer drug research. Moreover, an XP based Glide docking guided by different molecular modeling approaches led to rapid identification and initial optimization of novel series of CDK2 inhibitors.

Molecular mechanics based scoring methods using all atom force fields coupled MM-GBSA to model solvation have seen an upsurge in popularity. When compared to docking scoring functions, the physics-based methods provide improved correlation between calculated binding affinities and experimental data (Hou et al., 2011). In present study, remarkable results obtained with this methodology when compared to docking scoring functions, the MM-GBSA procedure provided more superior correlation between calculated binding free energies and biological activity of diverse set of CDK2 inhibitors. The notable results from MM-GBSA rescoring approach could be a more attractive alternative to the FEP and TI methodologies for rank-ordering. It can be as accurate approach to handle more structurally dissimilar ligands and more diverse set of pharmaceutically relevant targets, and structure-based lead optimization against CDK2 (Guimarães and Cardozo, 2008).

4. Conclusion

In this study, a combined computational approach was applied to gain insight into the structural basis and selectivity mechanism for three series of CDK2 inhibitors. We obtained several possible binding poses and an accurate ranking of binding affinities for three different series of CDK2 inhibitors using Glide XP docking and MM/GBSA-rescoring. This method reproduced the crystal structure precisely, and the docked results are consistent with the results from other studies. The docking simulations suggested modification to the 3,5-diaminoindazoles series with phenylacetyl type of substituents and cyclohexyl moiety of triazolo(1,5-*a*)pyridazines series of CDK2 inhibitors can show better inhibitory activity and to improve the pharmacokinetic profile of this class of compounds against CDK2. Thus it is representing a valuable tool for the structure-based design of future 3,5-diaminoindazoles and triazolo(1,5-*a*)pyridazines analogues. The hinge region and hydrophobic binding sites seem to be required for the optimum binding of novel CDK2 inhibitors. The MD simulations used here showed that complex formation between the inhibitors and CDK2 did not alter the enzyme structure to a significant extent. The predicted hydrogen bonds between the CDK2 and the inhibitors were restored in the energy minimized average structure of the complex. The calculated binding free energies were statistically significant in agreement with the biologically active diverse set of compounds and provide results at a fraction of the computational cost. These results obtained from the computational approach will be helpful for the structure based lead optimization and design of CDK2 inhibitors.

Acknowledgments

The authors thank the Department of Science and Technology New Delhi for Fast Track grant (SR/FT/CS-66/2010) and Alagappa University, Karaikudi for AURF (A13/BIF-AURF-2009) financial support for this study. One of the authors Sunil Kumar Tripathi gratefully acknowledges CSIR for the Senior Research Fellowship (9/688(0018)/12, EMR-I). The authors thank anonymous referee for the valuable suggestions.

Appendix A. Supporting information

Supplementary data associated with this article can be found in the online version at <http://dx.doi.org/10.1016/j.jtbi.2013.05.014>.

References

- Aixiao, L., Florent, B., Francois, M., Michel, D., Baoshan, W., 2008. Interaction mode and selectivity of the 2PU inhibitor with the CDK4 and CDK2 cyclin-dependant kinases: a molecular dynamics study. *J. Mol. Struct.: Theochem.* 849, 62–75.
- Alzate-Morales, J.H., Caballero, J., Vergara Jague, A., González Nilo, F.D., 2009. Insights into the structural basis of N2 and O6 substituted guanine derivatives as cyclin-dependent kinase 2 (CDK2) inhibitors: prediction of the binding modes and potency of the inhibitors by docking and ONIOM calculations. *J. Chem. Inf. Model.* 49, 886–899.
- Berendsen, H.J.C., Postma, J.P.M., Gunsteren, W.F.V., Hermans, J., 1981. Interaction models for water in relation to protein hydration. *Intermol. Forces* 11, 331–342.
- Berendsen, H.J.C., Postma, J.P.M., Vangunsteren, W.F., Dinola, A., Haak, J.R., 1984. Molecular-dynamics with coupling to an external bath. *J. Chem. Phys.* 81, 3684–3690.
- Berman, H.M., Westbrook, J., Feng, Z., Gilliland, G., Bhat, T.N., Weissig, H., Shindyalov, I.N., Bourne, P.E., 2000. The protein data bank. *Nucleic Acids Res.* 28, 235–242.
- Besson, A., Dowdy, S.F., Roberts, J.M., 2008. Cdk inhibitors: cell cycle regulators and beyond. *Dev. Cell* 14, 159–169.
- Blagden, S., de Bono, J., 2005. Drugging cell cycle kinases in cancer therapy. *Curr. Drug Targets* 6, 325–335.
- Bowers, K.J., Chow, E., Xu, H., Dror, R.O., Eastwood, M.P., Gregersen, B.A., Klepeis, J.L., Kolossvary, I., Moraes, M.A., Sacerdoti, F.D., Salmon, J.K., Shan, Y., Shaw, D.E., 2006a. Scalable Algorithms for Molecular Dynamics Simulations on Commodity Clusters, in: Proceedings of the ACM/IEEE Conference on Supercomputing (SC06), New York, NY: IEEE, 2006.
- Bowers, K.J., Dror, R.O., Shaw, D.E., 2007. Zonal methods for the parallel execution of range-limited N-body simulations. *J. Comput. Phys.* 221, 303–329.
- Bowers, K.J., Dror, R.O., Shaw, D.E., 2006b. The midpoint method for parallelization of particle simulations. *J. Chem. Phys.* 124, 184109–184111.
- Brandsdal, B.O., Österberg, F., Almlöf, M., Feierberg, I., Luzhkov, V.B., Åqvist, J., 2003. Free energy calculations and ligand binding. *Adv. Protein Chem.* 66, 123–158.
- Byth, K.F., Cooper, N., Culshaw, J.D., Heaton, D.W., Oakes, S.E., Minshull, C.A., Norman, R.A., Pauptit, R.A., Tucker, J.A., Breed, J., Pannifer, A., Rowsell, S., Stanway, J.J., Valentine, A.L., Thomas, A.P., 2004. Imidazo[1,2-*b*]pyridazines: a potent and selective class of cyclin-dependent kinase inhibitors. *Bioorg. Med. Chem. Lett.* 14, 2249–2252.
- Canavese, M., Santo, L., Raje, N., 2012. Cyclin dependent kinases in cancer: potential for therapeutic intervention. *Cancer Biol. Ther.* 13, 451–457.
- Child, E.S., Hendrychova, T., McCague, K., Futreal, A., Otyepka, M., Mann, D.J., 2010. A cancer-derived mutation in the pstaire helix of cyclin-dependent kinase 2 alters the stability of cyclin binding. *Biochim. Biophys. Acta Mol. Cell Res.* 1803, 858–864.
- Clare, P.M., Poorman, R.A., Kelley, L.C., Watenpaugh, K.D., Bannow, C.A., Leach, K.L., 2001. The cyclin-dependent kinases cdk2 and cdk5 act by a random, anti-cooperative kinetic mechanism. *J. Biol. Chem.* 276, 48292–48299.
- Das, D., Koh, Y., Tojo, Y., Ghosh, A.K., Mitsuya, H., 2009. Prediction of potency of protease inhibitors using free energy simulations with polarizable quantum mechanics-based ligand charges and a hybrid water model. *J. Chem. Inf. Model.* 49, 2851–2862.
- Davies, T.G., Bentley, J., Arris, C.E., Boyle, F.T., Curtin, N.J., Endicott, J.A., Gibson, A.E., Golding, B.T., Griffin, R.J., Hardcastle, I.R., Jewsbury, P., Johnson, L.N., Mesguiche, V., Newell, D.R., Noble, M.E.M., Tucker, J.A., Wang, L., Whitfield, H.J., 2002a. Structure based design of a potent purine-based cyclin-dependent kinase inhibitor. *Nat. Struct. Biol.* 9, 745–749.
- Davies, T.G., Pratt, D.J., Endicott, J.A., Johnson, L.N., Noble, M.E., 2002b. Structure-based design of cyclin-dependent kinase inhibitors. *Pharmacol. Ther.* 93, 125–133.
- De Azevedo, W.F., Leclerc, S., Meijer, L., Havlicek, L., Strnad, M., Kim, S.H., 1997. Inhibition of cyclin-dependent kinases by purine analogues-crystal structure of human cdk2 complexed with roscovitine. *Eur. J. Biochem.* 243, 518–526.

- De Azevedo, W.F., Mueller-Dieckman, H.J., Schulze-Gahmen, U., Worland, P.J., Sausville, E.A., Kim, S.H., 1996. Structural basis for specificity and potency of a flavonoid inhibitor of human cdk2, a cell cycle kinase. *Proc. Natl. Acad. Sci. USA* 93, 2735–2740.
- De Bondt, H.L., Rosenblatt, J., Jancarik, J., Jones, H.D., Morgan, D.O., Kim, S.H., 1993. Crystal structure of cyclin-dependent kinase 2. *Nature* 363, 595–602.
- Desmond, 2011. Version 3.0 Schrödinger, LLC, New York.
- Dessalew, N., Singh, S.K., 2008. 3D-QSAR CoMFA and CoMSIA study on benzodipyr-azoles as cyclin dependent kinase 2 inhibitors. *Med. Chem.* 4, 313–321.
- Dixon, J.S., Blaney, J.M., 1998. Docking: predicting the structure and binding affinity of ligand-receptor complexes. In: Martin, Y.C., Willet, P. (Eds.), *Designing Bioactive Molecules: Three-Dimensional Techniques and Applications*. American Chemical Society, Washington DC, pp. 175–198.
- Dror, O., Shulman-Peleg, A., Nussinov, R., Wolfson, H.J., 2004. Predicting molecular interactions in silico: I. A guide to pharmacophore identification and its applications to drug design. *Curr. Med. Chem.* 11, 71–90.
- Echalier, A., Endicott, J.A., Noble, M.E.M., 2010. Recent developments in cyclin-dependent kinase biochemical and structural studies. *Biochim. Biophys. Acta Proteins Proteomics* 1804, 511–519.
- Eldridge, M.D., Murray, C.W., Auton, T.R., Paolini, G.V., Mee, R.P., 1997. Empirical scoring functions: I. The development of a fast empirical scoring function to estimate the binding affinity of ligands in receptor complexes. *J. Comput. Aided. Mol. Des.* 11, 425–445.
- Englebienne, P., Fiaux, H., Kuntzm, D.A., Corbeil, C.R., Gerber-Lemaire, S., Rose, D.R., Moitessier, N., 2007. Evaluation of docking programs for predicting binding of Golgi alpha-mannosidase II inhibitors: a comparison with crystallography. *Proteins* 69, 160–176.
- Essmann, U., Perera, L., Berkowitz, M.L., Darden, T., Lee, H., Pedersen, L.G., 1995. A smooth particle meshes Ewald method. *J. Chem. Phys.* 103, 8577–8593.
- Friesner, R.A., Murphy, R.B., Repasky, M.P., Frye, L.L., Greenwood, J.R., Halgren, T.A., Sanschagrin, P.C., Mainz, D.T., 2006. Extra precision glide: docking and scoring incorporating a model of hydrophobic enclosure for protein–ligand complexes. *J. Med. Chem.* 49, 6177–6196.
- Friesner, R.A., Banks, J.L., Murphy, R.B., Halgren, T.A., Klicic, J.J., Mainz, D.T., Repasky, M.P., Knoll, E.H., Shelley, M., Perry, J.K., Shaw, D.E., Francis, P., Shenkin, P.S., 2004. Glide: a new approach for rapid, accurate docking and scoring. 1. Method and assessment of docking accuracy. *J. Med. Chem.* 47, 1739–1749.
- Furet, P., 2003. X-ray crystallographic studies of CDK2, a basis for cyclin-dependent kinase inhibitor design in anti-cancer drug research. *Curr. Med. Chem. Anticancer Agents* 3, 15–23.
- Furet, P., Meyer, T., Mittl, P., Fretz, H., 2001. Identification of cyclin-dependent kinase 1 inhibitors of a new chemical type by structure-based design and database searching. *J. Comput. Aided Mol. Des.* 15, 489–495.
- Glide, 2011. Version 5.7, Schrödinger, LLC, New York.
- Griffin, R., Henderson, A., Curtin, N., Echalié, A., Endicott, J., Hardcastle, L., Newell, D., Noble, M., Wang, L., Golding, B., 2006. Searching for cyclin-dependent kinase inhibitors using a new variant of the cope elimination. *J. Am. Chem. Soc.* 128, 6012–6013.
- Guimarães, C.R., Cardozo, M., 2008. MM-GB/SA rescoring of docking poses in structure-based lead optimization. *J. Chem. Inf. Model.* 48, 958–970.
- Halgren, T.A., Murphy, R.B., Friesner, R.A., Beard, H.S., Frye, L.L., Pollard, W.T., Banks, J.L., 2004. Glide: a new approach for rapid, accurate docking and scoring. 2. Enrichment factors in database screening. *J. Med. Chem.* 47, 1750–1759.
- Hayes, M.J., Stein, M., Weiser, J., 2004. Accurate calculations of ligand binding free energies. *J. Phys. Chem. A* 108, 3572–3580.
- Hou, T., Wang, J., Li, Y., Wang, W., 2011. Assessing the performance of the MM/PBSA and MM/GBSA methods. 1. The accuracy of binding free energy calculations based on molecular dynamics simulations. *J. Chem. Inf. Model.* 51, 69–82.
- Huo, S., Wang, J., Cieplak, P., Kollman, P.A., Kuntz, I.D., 2002. Molecular dynamics and free energy analyses of cathepsin D-inhibitor interactions: insight into structure-based ligand design. *J. Med. Chem.* 45, 1412–1419.
- Jiang, Y., Zou, J., Gui, C., 2005. Study of a ligand complexed with Cdk2/Cdk4 by computer simulation. *J. Mol. Model.* 11, 509–515.
- Johnson, L.N., 2009. Protein kinase inhibitors: contributions from structure to clinical compounds. *Q. Rev. Biophys.* 42, 1–40.
- Jorgensen, W.L., Maxwell, D.S., Tirado-Rives, J., 1996. Development and testing of the OPLS all-atom force field on conformational energetics and properties of organic liquids. *J. Am. Chem. Soc.* 118, 11225–11236.
- Kaminski, G.A., Friesner, R.A., Tirado-Rives, J., Jorgensen, W.L., 2001. Evaluation and reparametrization of the OPLS-AA force field for proteins via comparison with accurate quantum chemical calculations on peptides. *J. Phys. Chem. B* 105, 6474–6487.
- Karplus, M., McCammon, J.A., 2002. Molecular dynamics simulations of biomolecules. *Nat. Struct. Biol.* 9, 646–652.
- Kitchen, D.B., Decornez, H., Furr, J.R., Bajorath, J., 2004. Docking and scoring in virtual screening for drug discovery: methods and applications. *Nat. Rev. Drug Discov.* 3, 935–949.
- Koh, Y., Das, D., Leschenko, S., Nakata, H., Ogata-Aoki, H., Amano, M., Nakayama, M., Ghosh, A.K., Mitsuya, H., 2009. GRL-02031, a novel nonpeptidic protease inhibitor (PI) containing a stereochemically defined fused cyclopentanyltetrahydrofuran potent against multi-PI-resistant human immunodeficiency virus type 1 In Vitro. *Antimicrob. Agents Chemother.* 53, 997–1006.
- Kroemer, R.T., Vulpetti, A., McDonald, J.J., Rohrer, D.C., Trosset, J.Y., Giordanetto, F., Cotesta, S., McMartin, C., Kihlén, M., Stouten, P.F., 2004. Assessment of docking poses: interactions-based accuracy classification (IBAC) versus crystal structure deviations. *J. Chem. Inf. Comput. Sci.* 44, 871–881.
- Kumar, N., Hendriks, B.S., Janes, K.A., de Graaf, D., Lauffenburger, D.A., 2006. Applying computational modeling to drug discovery and development. *Drug Discov. Today* 11, 806–811.
- Lee, J., Choi, H., Kim, K.H., Jeong, S., Park, J.W., Baek, C.S., Lee, S.H., 2008. Synthesis and biological evaluation of 3,5-diaminoindazoles as cyclin-dependent kinase inhibitors. *Bioorg. Med. Chem. Lett.* 18, 2292–2295.
- Legraverend, M., Tunnah, P., Noble, M., Ducrot, P., Ludwig, O., Grierson, D.S., Leost, M., Meijer, L., Endicott, J., 2000. Cyclin-dependent kinase inhibition by new C-2 alkynylated purine derivatives and molecular structure of a CDK2-inhibitor complex. *J. Med. Chem.* 43, 1282–1292.
- LigPrep, 2011. Version 2.5, Schrödinger, LLC, New York.
- Lin, J.H., Perryman, A.L., Schames, J.R., McCammon, J.A., 2002. Computational drug design accommodating receptor flexibility: the relaxed complex scheme. *J. Am. Chem. Soc.* 124, 5632–5633.
- Lyne, P.D., Lamb, M.L., Saeh, J.C., 2006. Accurate prediction of the relative potencies of members of a series of kinase inhibitors using molecular docking and MM-GBSA scoring. *J. Med. Chem.* 49, 4805–4808.
- Malumbres, M., Barbacid, M., 2009. Cell cycle, cdks and cancer: a changing paradigm. *Nat. Rev. Cancer* 9, 153–166.
- Mani, S., Wang, C., Wu, K., Francis, R., Pestell, R., 2000. Cyclin-dependent kinase inhibitors: novel anticancer agents. *Exp. Opin. Invest. Drugs* 9, 1849–1870.
- Martyna, G.J., Klein, M.L., Tuckerman, M., 1992. Nose–Hoover chains—the canonical ensemble via continuous dynamics. *J. Chem. Phys.* 97, 2635–2643.
- Martyna, G.J., Tobias, D.J., Klein, M.L., 1994. Constant-pressure molecular dynamics algorithms. *J. Chem. Phys.* 101, 4177–4189.
- McGaughey, G.B., Gagne, M., Rappe, A.K., 1998. π -Stacking Interactions alive and well in proteins. *J. Biol. Chem.* 273, 15458–15463.
- Meijer, L., Raymond, E., 2003. Roscovitine and other purines as kinase inhibitors. From starfish oocytes to clinical trials. *Acc. Chem. Res.* 36, 417–425.
- Morgan, D.O., 1997. Cyclin-dependent kinases: engines, clocks, and microprocessors. *Annu. Rev. Cell Dev. Biol.* 13, 261–291.
- Norberg, J., Nilsson, L., 2003. Advances in biomolecular simulations: methodology and recent applications. *Q. Rev. Biophys.* 36, 257–306.
- Onodera, K., Satou, K., Hirota, H., 2007. Evaluations of molecular docking programs for virtual screening. *J. Chem. Inf. Model.* 47, 1609–1618.
- Otyepka, M., Krystof, V., Havlicek, L., Siglerova, V., Strnad, M., Koca, J., 2000. Docking-based development of purine-like inhibitors of cyclin-dependent kinase2. *J. Med. Chem.* 43, 2506–2513.
- Perola, E., Walters, W.P., Charifson, P.S., 2004. A detailed comparison of current docking and scoring methods on systems of pharmaceutical relevance. *Proteins* 56, 235–249.
- Prime, 2011. Version 3.0 Schrödinger, LLC, New York.
- Rapp, C., Kalyanaraman, C., Schiffmiller, A., Schoenbrun, E.L., Jacobson, M.P., 2011. A molecular mechanics approach to modeling protein–ligand interactions: relative binding affinities in congeneric series. *J. Chem. Inf. Model.* 51, 2082–2089.
- Richardson, C.M., Williamson, D.S., Parratt, M.J., Borgognoni, J., Cansfield, A.D., Dokurno, P., Francis, G.L., Howes, R., Moore, J.D., Murray, J.B., Robertson, A., Surgenor, A.E., Torrance, C.J., 2006. Triazololo[1,5-*a*]pyrimidines as novel CDK2 inhibitors: protein structure-guided design and SAR. *Bioorg. Med. Chem. Lett.* 16, 1353–1357.
- Rosania, G.R., Chang, Y.T., 2000. Targeting hyperproliferative disorders with cyclin dependent kinase inhibitors. *Exp. Opin. Ther. Patents* 10, 215–230.
- Russo, A.A., Jeffrey, P.D., Patten, A.K., Massagué, J., Pavletich, N.P., 1996. Crystal structure of the p27Kip1 cyclin-dependent-kinase inhibitor bound to the cyclin A-Cdk2 complex. *Nature* 382, 325–331.
- Ryckaert, J.P., Ciccotti, G., Berendsen, H.J.C., 1977. Numerical-integration of cartesian equations of motion of a system with constraints—molecular dynamics of N-alkanes. *J. Comput. Phys.* 23, 327–341.
- Schames, J.R., Henchman, R.H., Siegel, J.S., Sotriffer, C.A., Ni, H., McCammon, J.A., 2004. Discovery of a novel binding trench in HIV integrase. *J. Med. Chem.* 47, 1879–1881.
- Schneidman-Duhovny, D., Nussinov, R., Wolfson, H.J., 2004. Predicting molecular interactions in silico: II. Protein–protein and protein–drug docking. *Curr. Med. Chem.* 11, pp. 91–107.
- Shaw, D.E., 2005. A fast, scalable method for the parallel evaluation of distance-limited pairwise particle interactions. *J. Comput. Chem.* 26, 1318–1328.
- Singh, S.K., Tripathi, S.K., Dessalew, N., Singh, P., 2012. Cyclin Dependent Kinase as Significant Target for Cancer Treatment. *Curr. Cancer Ther. Rev.* 8, 225–235.
- Sinnokrot, M.O., Valeev, E.F., Sherrill, C.D., 2002. Estimates of the ab initio limit for pi–pi interactions: the benzene dimer. *J. Am. Chem. Soc.* 124, 10887–10893.
- Talele, T.T., McLaughlin, M.L., 2008. Molecular docking/dynamics studies of Aurora A kinase inhibitors. *J. Mol. Graph. Model.* 26, 1213–1222.
- Tetsu, O., McCormick, F., 2003. Proliferation of cancer cells despite cdk2 inhibition. *Cancer Cell* 3, 233–245.
- Tripathi, S.K., Singh, S.K., Singh, P., Chellaperumal, P., Reddy, K.K., Selvaraj, C., 2012. Exploring the selectivity of a ligand complex with CDK2/CDK1: a molecular dynamics simulation approach. *J. Mol. Recognition* 25, 504–512.
- Vadivelan, S., Sinha, B.N., Irudayam, S.J., Jagarlapudi, S.A.R.P., 2007. Virtual screening studies to design potent cdk2–cyclin inhibitors. *J. Chem. Inf. Model.* 47, 1526–1535.
- Wang, J., Dixon, R., Kollman, P.A., 1999. Ranking ligand binding affinities with avidin: a molecular dynamics-based interaction energy study. *Proteins* 34, 69–81.
- Zhou, Z., Felts, A.K., Friesner, R.A., Levy, R.M., 2007. Comparative performance of several flexible docking programs and scoring functions: enrichment studies for a diverse set of pharmaceutically relevant targets. *J. Chem. Inf. Model.* 47, 1599–1608.